Available online at www.sciencedirect.com
SCIENCE DIRECT®
Journal of Power Sources 137 (2004) 62–70
JOURNAL OF POWER SOURCES
www.elsevier.com/locate/jpowsour

Dissolution behavior of Co-coated NiO cathode in molten $(Li_{0.62}K_{0.38})_2CO_3$ eutectics

B.H. Ryu [a,b], J. Han [a,*], S.P. Yoon [a], S.W. Nam [a], T.-H. Lim [a], S.-A. Hong [a], K.B. Kim [b]

[a] *Fuel Cell Research Center, Korea Institute of Science & Technology, Seoul 130-650, South Korea*
[b] *Department of Metallurgical Engineering, Yonsei University, 134 Sinchon-dong, Seodamun-gu, Seoul, South Korea*

Received 26 April 2004; accepted 21 May 2004
Available online 13 August 2004

Abstract

The dissolution behavior of the NiO–CoO electrodes in molten $(Li_{0.62}K_{0.38})_2CO_3$ eutectics as a function of Co content was investigated under the standard cathodic gas composition at 650 °C. In order to prepare NiO–CoO electrodes, Co was deposited on the porous Ni electrode using galvanostatic pulse plating technique followed by the oxidation process. Compared to the pure NiO electrode, NiO–CoO electrodes showed low Ni solubility in molten $(Li_{0.62}K_{0.38})_2CO_3$ eutectics. Solubility of NiO–CoO electrodes depended on the partial pressure of carbon dioxide (P_{CO_2}) and the Ni solubility increased with P_{CO_2}. On the other hand, the Ni solubility was not affected by the partial pressure of oxygen (P_{O_2}). The XRD analysis after the dissolution experiment, showed that the Ni solubility decreased with increase of the amount of lithium incorporated in the electrodes and that the lithium incorporation was promoted by the formation of NiO–CoO solid solution. The results obtained in the present study suggested that NiO–CoO solid solution could effectively suppress the NiO dissolution in the molten $(Li_{0.62}K_{0.38})_2CO_3$ eutectics.

Keywords: NiO dissolution; Galvanostatic pulse plating; Co; MCFC; Cathode

1. Introduction

Lithiated NiO is the commonly used material for the cathode in molten carbonate fuel cell (MCFC) because of its high electrode activity [1]. However, the long-term stability of the NiO cathode has not been considered good enough to meet the commercialization requirement of 40,000 h operation. It is mainly because of NiO dissolution into the molten carbonates, which causes a short-circuit of the cell. In order to overcome NiO dissolution, several different methods have been proposed by many research groups in the world. One of the methods to suppress the NiO dissolution is the addition of additives, such as alkali earth metal oxide [2,3], Co [4–7], Fe [8], Nb [9,10], Ce [11,12] and lanthanum oxide [13–15] into the NiO and/or the molten carbonate salt. The addition of these additives increases the basicity of the electrolyte and, thus, suppresses the NiO dissolution that follows the acidic dissolution mechanism. However, the addition of the additives has not been appreciable to the cathode modification because these additives cause the degradation of the electrical conductivity during long-term operation [3].

The other suppression method is the development of new cathode materials such as $LiCoO_2$, $LiFeO_2$ [16–20]. Alternative cathode materials mentioned above showed higher stability in molten carbonate salts than the pure NiO, but their electrical conductivity were lower than that of NiO [16]. Moreover, it was difficult to fabricate the cathode in the size over 1 m^2 using these alternative materials because of the difficulties in sintering process.

Recently, a prospective method for suppression of NiO dissolution has been reported by the present laboratory [21,22]. In this novel method, a porous Ni electrode was coated with stable materials, such as $LiCoO_2$ and $LiCo_{1-x}Ni_xO_2$. This coating method effectively suppressed the NiO dissolution without degradation in electrical conductivity of the cathode. In addition, this method could prepare the cathode in large size without serious change in the fabrication process. Since we have reported this novel method, many other research groups have reported NiO dissolution behavior of the Co (or $LiCoO_2$)-coated electrodes prepared by various coating techniques such as sol–gel [23], electroless plating [24], and mechanical coating [4–6]. All of these coated NiO electrodes, regardless of the fabrication

* Corresponding author. Present address: 39-1 Hawolgok-dong, Seongbuk-gu, Fuel Cell Research Center, KIST, Seoul 136-791, South Korea. Tel.: +81 2 958 5277; fax: +81 2 958 5199.
E-mail address: jhan@kist.re.kr (J. Han).

0378-7753/$ – see front matter © 2004 Elsevier B.V. All rights reserved.
doi:10.1016/j.jpowsour.2004.05.037

technique, yield lower NiO solubility in the molten carbonate salt than that of the pure NiO electrode. Although many research groups have studied this method intensively, the mechanism for the suppression of the NiO dissolution by a coating layer was not clear.

In the present study, the NiO–CoO electrodes with various Co contents were prepared by the galvanic pulse plating method and the Ni solubility of the prepared electrodes were measured by dissolution experiments. The mechanism of the dissolution suppression by Co-coating has been investigated using various characterization methods, such as XRD.

2. Experimental

2.1. Samples preparation

In order to prepare NiO–CoO electrodes with various Co contents, Co was deposited on the porous Ni electrode using the galvanic pulse plating method. The apparatus used in the pulse plating system consisted of a pulse generator, water bath and electroplating bath. The pulse generator was HC-112 of Hokuto Denko Ltd., which had a power source and pulse generator system. Galvanostatic pulse plating was performed in the electroplating bath surrounded by water bath held at 30 °C. The anode was a dual Pt/Ti mesh and the cathode was a state of the art porous Ni electrode with porosity 80% prepared by tape casting. The effective area of a cathode was 24 cm^2 (3 cm × 4 cm × 0.075 cm × 2). In order to obtain a homogeneous Co coating layer, pulse on-time (T_{on}) and off-time (T_{off}) was determined by the calculation method shown by Puppe et al. [25]. According to the authors, pulse-on time (T_{on}) was longer than the charging time and pulse-off time (T_{off}) was seven times larger than T_{on} for inhibiting the damping of faradic current. Therefore, pulse on-time (T_{on}) and pulse off-time (T_{off}), under the assumption of double layer capacitance (C) of 50 μF/cm^2, was calculated as:

$$\text{pulse on time } (T_{on}) \geq \frac{17}{J_p}, \quad \text{pulse off time } (T_{off}) \geq \frac{120}{J_p} \tag{1}$$

where T_{on} and T_{off} are pulse-on and off-time in microsecond, respectively and J_p indicates pulse current density in A/cm^2. By this calculation method, the duty cycle, T_{on} and T_{off} were calculated as 0.125, 100 and 700 μs, respectively.

The bath solution was prepared by dissolving cobalt sulfate (330 g/l), cobalt chloride (45 g/l) and boric acid (30 g/l) into distilled water. The pH value of the bath solution was controlled by sulfuric acid. Two different bath solutions with different pH values were prepared and the bath solutions with pH 2 and pH 4 were designated as S1 and S2, respectively. To obtain the desired Co content, current efficiency was determined by Faraday's law of weight gain, which was 53 and 65% for the samples prepared in the bath solutions with pH 2–4, respectively. Various samples with different Co content between 2 and 12 wt.% of Co were prepared by a change in the plating time. After the plating process, the prepared samples were oxidized at 750 °C for 5 h in air atmosphere in order to obtain NiO–CoO electrodes.

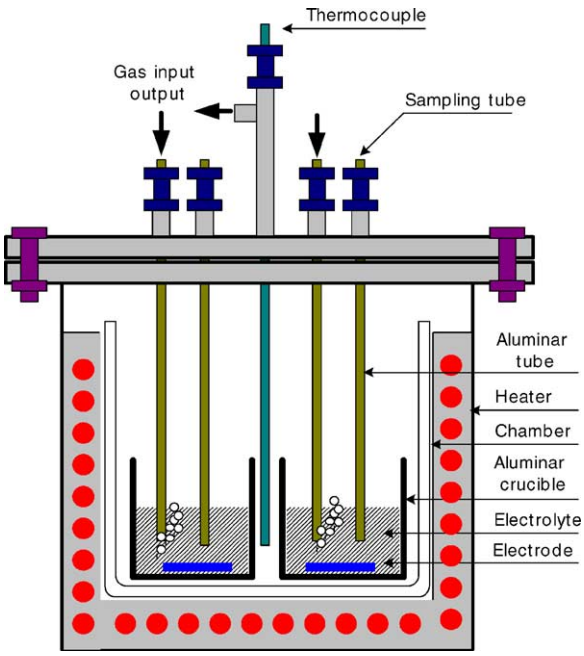

Fig. 1. Schematic illustration of pot cell system for dissolution experiment.

2.2. NiO dissolution experiment

The solubility of the NiO–CoO electrodes was evaluated in the home-built pot cell system. As shown in Fig. 1, the pot cell system consisted of a sample chamber, a gas delivery system and a temperature control system. The sample chamber, made of AISI 316L, was placed in the tubular furnace and the temperature inside the sample chamber was controlled by the thermocouple and the tubular furnace. Three alumina crucibles were placed in the sample chamber and they were used as sample containers. The sample chamber was sealed with O-rings in order to separate the chamber from the ambient air and to control the gas composition in the chamber. The gas was supplied through three long alumina tubes. The one end of the alumina tubes was immersed into the carbonate melt in order to bubble the carbonate melts with gas. The flow rate of the gas was controlled by mass flow controllers.

Prior to the solubility measurement, 62 mol% Li_2CO_3 + 38 mol% K_2CO_3 eutectic was purified in the pot cell system at 700 °C under CO_2 environment [26]. The purified carbonate was placed in the alumina crucibles in the sample chamber and the sample chamber was slowly heated up. When the temperature in the chamber reached to 650 °C, the prepared NiO–CoO electrodes were immersed into the carbonate melt. Then, the sample chamber was

closed and the mixed gas of oxygen (0.33 atm) and carbon dioxide (0.67 atm) was delivered into the chamber through the mass flow controller. A small amount of the carbonate melt (0.2–0.5 g) was taken out periodically using a pure alumina tube through the holes on the lid of the sample chamber. The sampled carbonate melt was dissolved in 10 vol.% acetic acid. Then, fine oxide particles in the solution were eliminated by filter paper. Ionic concentrations in the filtered solution were measured by the atomic absorption spectroscopy (AAS) and the solubility was estimated by the constant concentration of Ni and Co cations [27].

2.3. Characterization of the prepared electrode

In order to examine the characteristics of the prepared sample electrodes, several different analysis techniques were employed. Surface morphology and Co distribution along with the depth direction of porous Ni electrode were explored by scanning electron microscopy (Philips XL30 ESEM) coupled with energy dispersive spectrometry (EDAX). The phase structures of electrodes were characterized by XRD (Rigaku RINT-5200) equipped with a thin film attachment using Cu Kα radiation. To compensate the translation and dilation of X-ray peaks, silicon powder (single crystal wafer, space group, *Fd*3*m*) was spread on the surface of electrodes.

3. Results and discussion

3.1. Characteristics of Co-plated electrodes

Co was plated on to porous Ni electrodes various mean current densities and with pH values of the bath solution

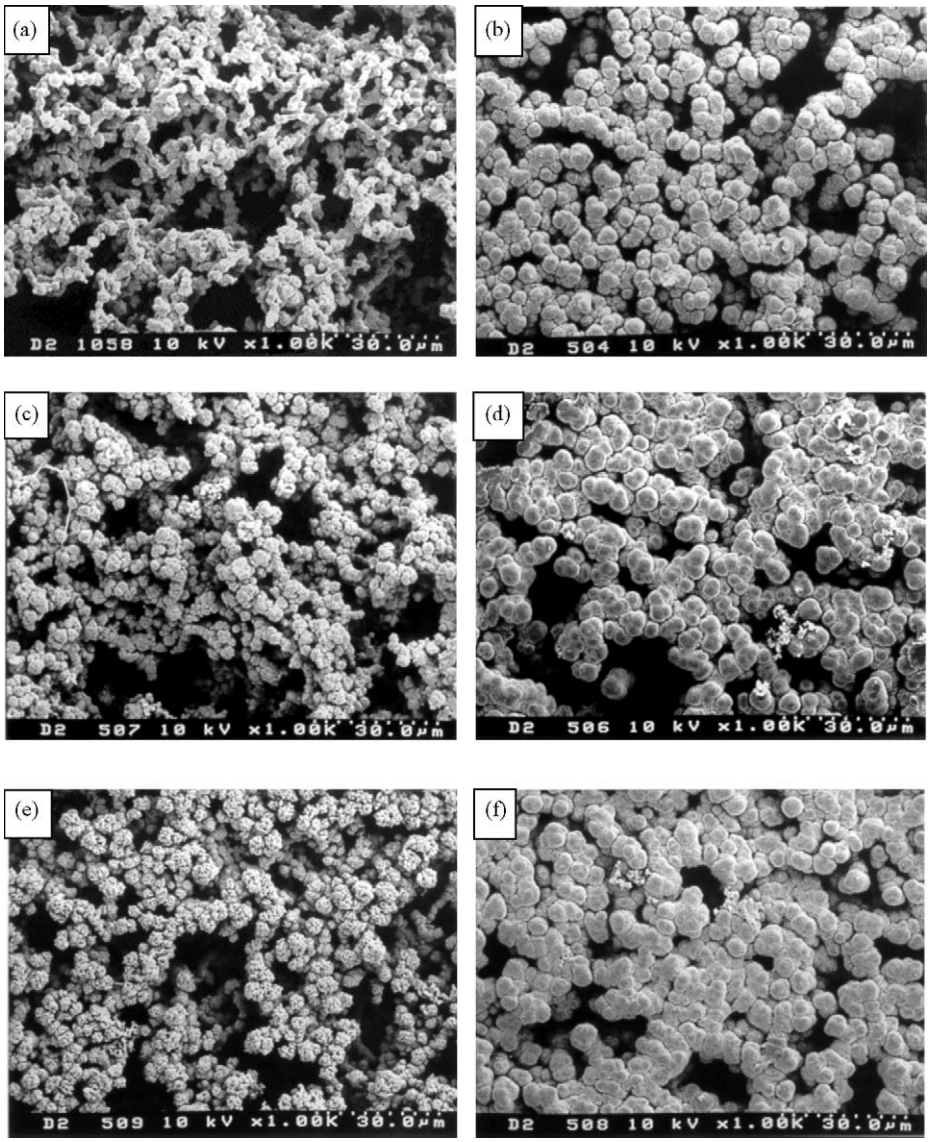

Fig. 2. SEM images of porous nickel obtained by Co pulse plating for 6 min; (a) as-received, (b) 100 mA/cm^2 at pH 4, (c) 200 mA/cm^2 at pH 2, (d) 200 mA/cm^2 at pH 4, (e) 400 mA/cm^2 at pH 2, (f) 400 mA/cm^2 at pH 4.

by galvanostatic pulse plating technique and the surface morphologies of the resulting electrodes are investigated by scanning electron microscopy (SEM). The SEM images of the surface of the prepared electrodes were presented in Fig. 2. It was confirmed by the SEM images that Co was plated successfully on the surface of Ni particles, but the surface morphologies of the Co-coated Ni electrodes were different with the plating conditions. Fig. 2(a) shows the surface of the porous Ni electrode without Co plating. The images on the left hand side (Fig. 2(c) and (e)) are the surface images of the electrodes prepared in the bath solution of S1 and those on the right hand side (Fig. 2(b), (d) and (f)) show the surface of the electrodes prepared in the bath solution S2. The comparison, the electrodes shown in Fig. 2 were plated with Co for 6 min. As shown in the figure, more Co was plated on the Ni particles when a higher mean current density was applied. Also, the electrodes plated in the bath solution of S2 with pH 4 [Fig. 2(b), (d) and (f)] showed much more Co plated on the Ni particles and the growth of the Co layer on the Ni particles led to the reduction of pore volume. On the other hand, the electrodes plated in the bath solution of S1 with pH 2 (Fig. 2(c) and (e)) did not show significant change in pore structure. Also, the Co layer plated in the bath solution S1, consisted of small primary particles, while the Co layer plated in the bath solution S2 looked like films grown on the surface of Ni particles. According to Bai and Hu [28], the formation of small nuclei was accelerated in the bath solution with a low pH value by the hydrogen evolution reaction (HER). Similar to their results, small Co particles were grown on the small nuclei formed on the surface of Ni particles in the bath solution S1 with low pH value in the present case.

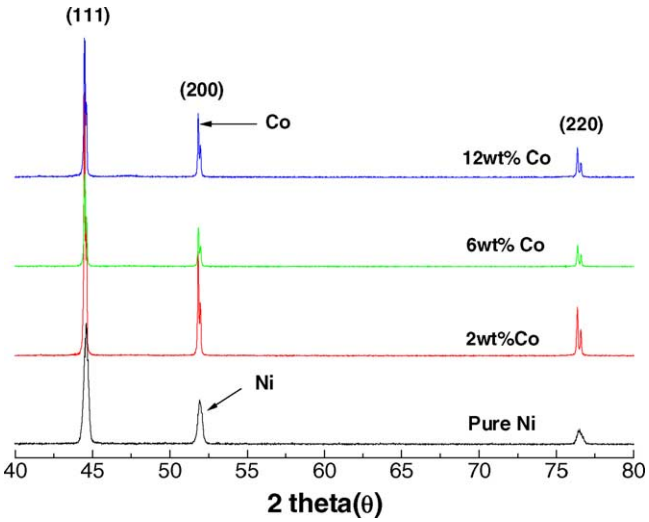

Fig. 4. XRD patterns of Co-coated Ni electrode at 300 mA/cm^2 under bath pH = 2.

Co distributions along with the depth direction of the porous Ni electrodes were investigated by Co mapping of EDAX and the results are presented in Fig. 3. Although a large amount of Co was found on the surface of the electrodes plated in the bath solution S2, no Co was found deep inside the electrodes. Most Co was plated on the surface of the porous Ni electrodes and the penetration depth was less than 30 μm in the electrodes prepared in the bath solution

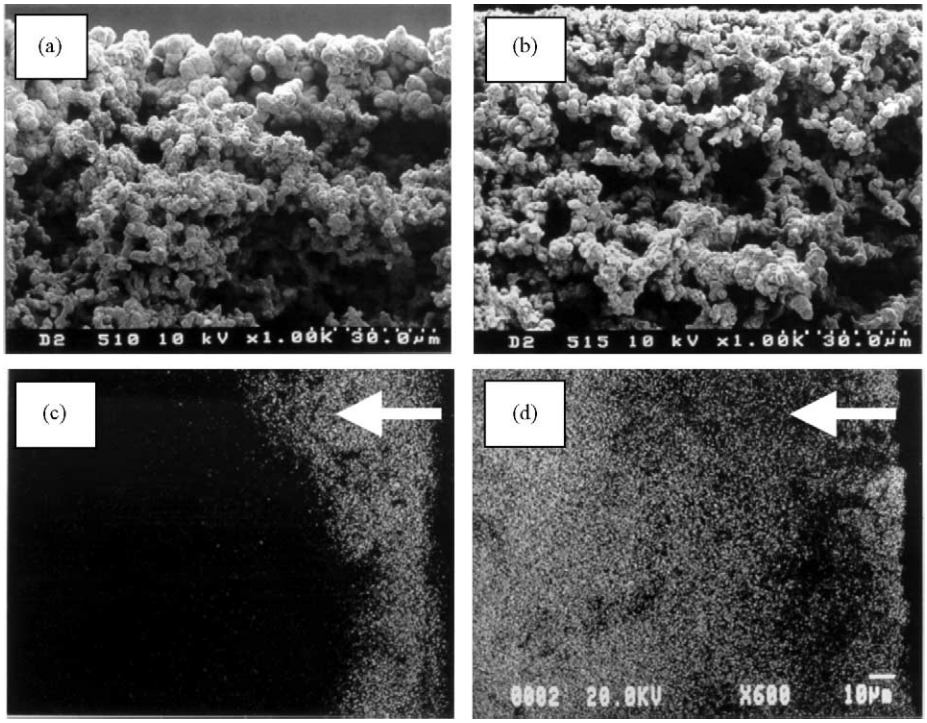

Fig. 3. EDAX image of Co through the cross section of porous nickel; (a, c) 100 mA/cm^2, pH 4, (b, d) 100 mA/cm^2, pH 2.

S2. On the other hand, homogeneous Co distribution was found, even in the deep inside of electrodes, in the electrodes prepared in the bath solution S1. In the case of the electrodes prepared in the bath solution S1, the penetration depth was more than 120 μm. Consequently, the electrodes plated in the bath solution S1 with low pH value showed homogeneous Co distribution along the depth direction and thus, the electrodes prepared for the solubility evaluation experiment in the present study were prepared using the bath solution S1.

Fig. 4 shows typical XRD profiles of the porous Ni electrode and Co-coated Ni electrodes prepared at 100 mA/cm of mean current density in the bath solution S1. The XRD profiles confirm that metallic Co was successfully plated on the porous Ni electrodes and that the plated Co layer had the face centered cubic (FCC) phase. According to Barrera et al. [29], cubic phased Co was plated in the bath solution with a pH value lower than 4 and the electrodes prepared in the present study showed consistent results. The cubic structure of the plated Co layer was considered advantageous for the oxidation process because it is easy for Ni and Co with the same phase structure to be oxidized in the form of a solid solution.

The prepared electrodes were oxidized at 750 °C for 5 h in the air atmosphere. Typical XRD profiles of the oxidized electrodes are presented in Fig. 5. For calibration the silicon powder was spread on the surface of the electrode resulting in the appearance of Si peaks in the XRD profile in Fig. 5. After the oxidation process, the electrodes with Co content less than 6 wt.% formed NiO–CoO solid solutions. On the other hand, the electrodes with Co contents higher than 6 wt.% showed Co_3O_4 peaks as well as solid solution peaks. In order to quantify the amount of Co_3O_4, the cubic lattice constants were calculated from the XRD profiles by the least square method and the amount of CoO in the solid solution were calculated by the Vegard's law. The lattice constants of the NiO and CoO used in the calculation were 4.177 and 4.262 Å, respectively [30,31] and the calculated results are presented in Table 1. As shown in the table, less than 0.1% of Co turned into Co_3O_4 and most of Co formed the solid solution with NiO. Thus, the oxidation process could be considered effective for preparing electrodes of NiO–CoO solid solutions.

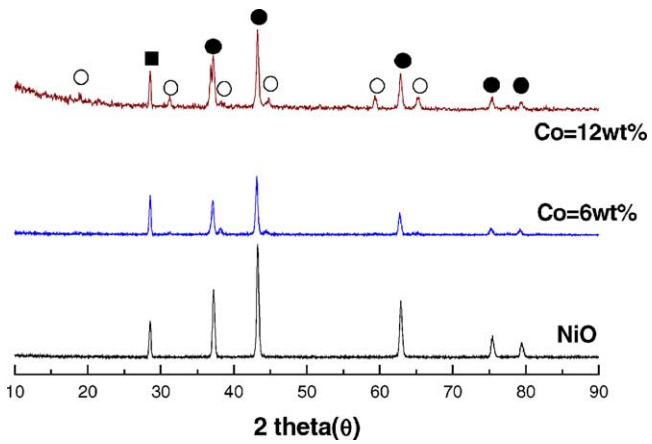

Fig. 5. XRD profiles of NiO and NiO–CoO electrodes after oxidation; (Co, Ni)O (●), Si (■), Co_3O_4 (○).

3.2. NiO dissolution and solubility

The solubilities of NiO and NiO–CoO electrodes prepared in the present study were estimated by a dissolution experiment. Fig. 6(a) shows the variation of the mole fraction of Ni in the molten $(Li_{0.62}/K_{0.38})_2CO_3$ eutectics as a function of immersion time at 650 °C. As shown in the figure, the Ni mole fraction for all NiO and NiO–CoO electrodes increased significantly at the initial stage of the experiment and reached a constant value after 100 h. Thus, the constant Ni mole fraction obtained after 100 h could be considered as an equilibrium value and this value is, in general, regarded as the Ni solubility of the electrodes. In the present study, the solubility of the electrodes in the molten carbonate is

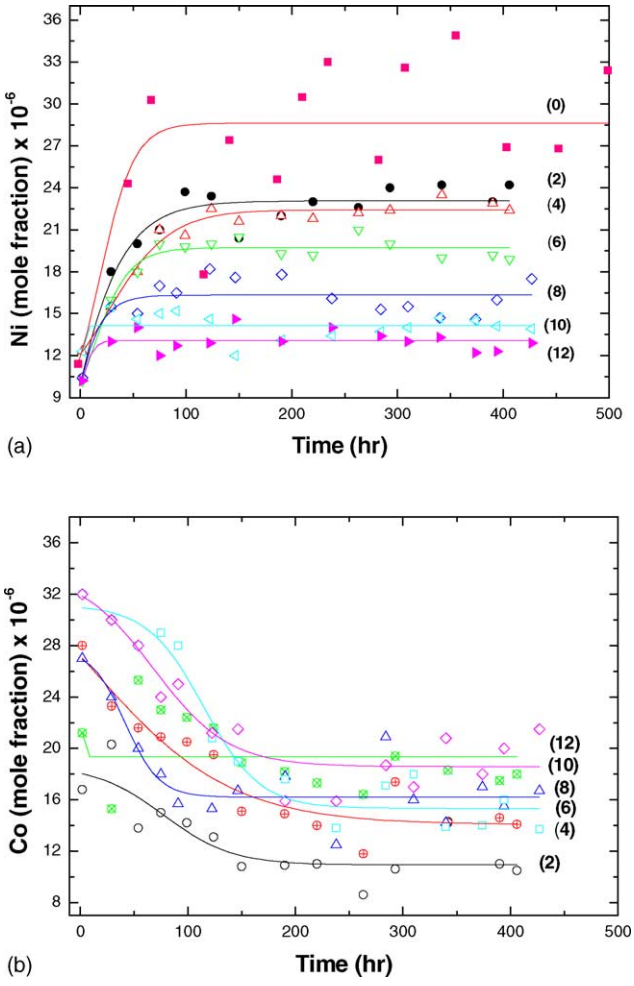

Fig. 6. Time dependency of ions mole fraction; Ni (a) and cobalt (b) in molten $Li_{0.62}/K_{0.38}$ carbonate eutectics at 923 K under 1 atm, the numbers in brackets are the amount of Co in NiO–CoO electrodes.

Table 1
Co contents in CoO-NiO solid solution and Co_3O_4 calculated by Vegard's law

Co content in Co-coated Ni electrode (wt.%)	Co content in NiO–CoO solid solution after oxidation (wt.%)	Co content in Co_3O_4	Ratio of Co in solid solution to Co in Co_3O_4 (wt.%)
6	6	0	100
8	7.998	0.002	99.975
10	9.995	0.005	99.950
12	11.989	0.011	99.908

also defined as the constant Ni mole fraction.

The solubility of the NiO electrode in molten carbonate at 650 °C was about 30×10^{-6} and this is consistent with the previous results in the literature [32]. On the other hand, the Ni solubilities of NiO–CoO electrodes were much lower than that of NiO electrode, and decreased with increase of Co content. The lowest Ni solubility was measured with the NiO–CoO electrode of 12 wt.% Co and the solubility was about 13×10^{-6}. This solubility was less than half of the solubility of the NiO electrode and it confirms that NiO–CoO electrodes had the potential for solving the NiO dissolution problems in MCFC.

Fig. 6(b) shows the variation of Co mole fraction of NiO–CoO electrodes. The Co mole fraction of NiO–CoO electrodes in molten carbonate decreased with immersion time at the initial stage and reached equilibrium after 150 h. The Co solubilities measured in this study were in the range between 10 and 12×10^{-6} and these are much higher than that in the literature [4–6]. According to Fukui et al. [4–6], Co solubility was 1×10^{-6} under the gas mixture of CO_2 and air (30/70). However, the experimental conditions of Fukui et al. were different from those used in the present study.

The solubilities of the NiO and NiO–CoO electrodes were measured as a function of the partial pressures of CO_2 (P_{CO_2}) and O_2 (P_{O_2}). The partial pressures of the supplied gases were changed in the range of 0.1–0.67 atm with the fixed partial pressure of the other gas at 0.33 atm and the total pressure was balanced at 1atm using nitrogen. The variation of the solubilities with P_{CO_2} and P_{O_2} are presented in Fig. 7 (a) and (b), respectively. As shown in the Fig 7(a), the Ni solubilities of NiO and NiO–CoO electrodes increased with P_{CO_2}, while the Ni solubilities of NiO and NiO–CoO of electrodes did not change with P_{O_2}. As in the literature [33,34], this results implied that Ni dissolution in the molten $(Li_{0.62}/K_{0.38})_2CO_3$ eutectics at the present conditions followed the acidic dissolution mechanism.

The solid lines in Fig. 7(a) show the results of linear regression and the slope of the plot could be considered as the sensitivity of the Ni solubility on P_{CO_2}. It was clearly observed that the slope of the NiO electrode was larger than those of NiO–CoO electrodes. Thus, it could be concluded that NiO–CoO electrodes are more stable than the NiO electrode in the molten $(Li_{0.62}/K_{0.38})_2CO_3$ eutectics in the respect of NiO dissolution.

Fig. 8 showed the dependency of Co solubilities of NiO–CoO electrodes on the partial pressure. Co solubilities also increased with the increase of P_{CO_2}, but not with P_{O_2}. This also indicates that the Co dissolution of NiO–CoO electrodes followed the acidic dissolution mechanism in the molten $(Li_{0.62}K_{0.38})_2CO_3$ eutectics.

3.3. Post-test analysis

As shown above, NiO dissolution is strongly affected by the partial pressure of carbon dioxide (P_{CO_2}) and the composition of the electrodes. In order to investigate the role of Co in the suppression of NiO dissolution in the molten

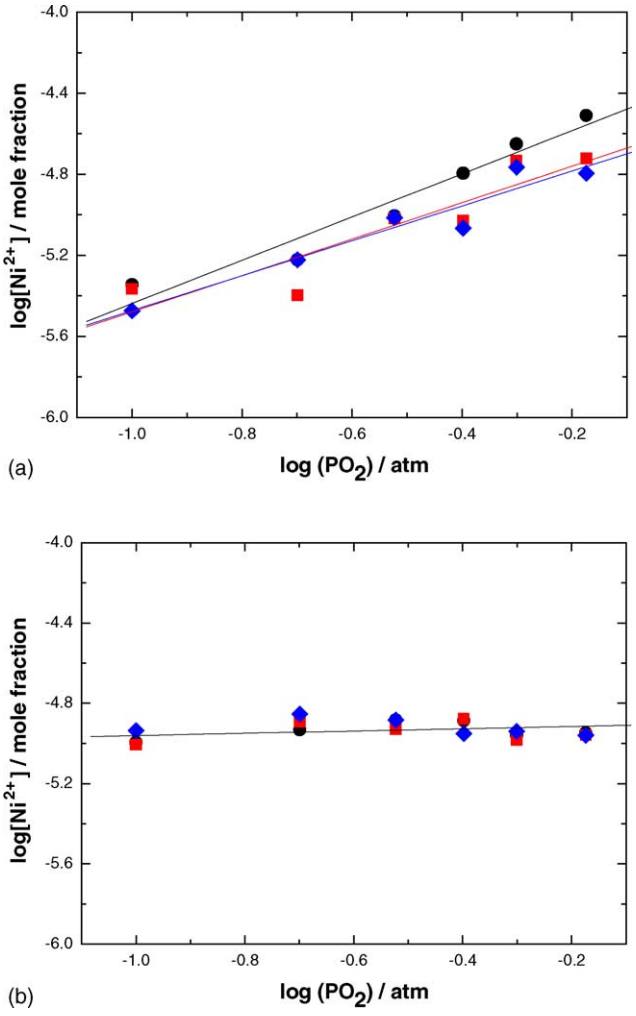

Fig. 7. Ni Solubility of the pure NiO cathode and NiO–CoO electrodes as a function of the partial pressure of carbon dioxide (a), oxygen (b); (●) NiO,(■) 6 wt.% Co, (◆) 12 wt.% Co.

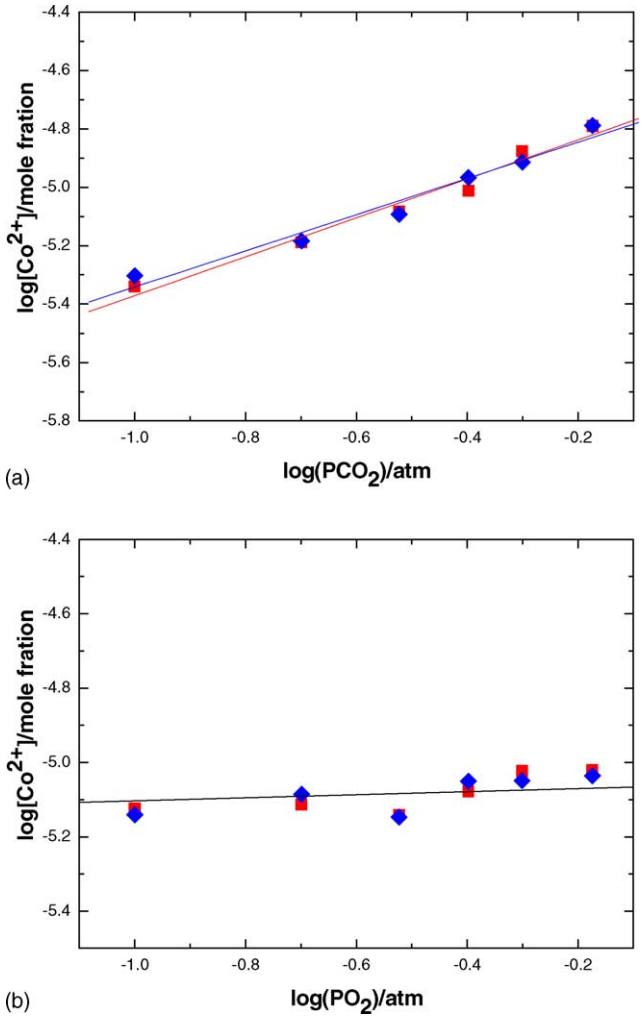

Fig. 8. Co Solubility of NiO–CoO electrodes as a function of the partial pressure of carbon dioxide (a), oxygen (b); (■) 6 wt.% Co, (◆) 12 wt.% Co.

$(Li_{0.62}/K_{0.38})_2CO_3$ eutectics, all electrodes were analyzed by several characterization tools after the dissolution experiment.

Fig. 9 presents the SEM micro images showing the morphology of NiO and NiO–CoO electrodes after the dissolution experiment. As shown in the figure, crystallites were grown on the particle surface of the NiO and the NiO–CoO electrodes. The size of the crystallites in the NiO–CoO electrodes with Co contents of 6 and 12 wt.% were about 0.3 and 0.7 μm, respectively. Therefore, it could be considered that the crystallites grown on the particle surface of NiO–CoO electrodes are related to Co and the crystallites should be Li–Ni–Co–O compounds.

In order to verify the phase structure of the crystallites grown on the particle surface of NiO–CoO electrodes, the XRD analysis of thin film mode was carried out and the XRD profiles are shown in Fig. 10. In the XRD profiles of the NiO electrode, peaks for cubic phased Li–Ni–O compound were observed as expected. In the XRD profiles of NiO–CoO electrodes, peaks of Li–Co–Ni–O compound were found,

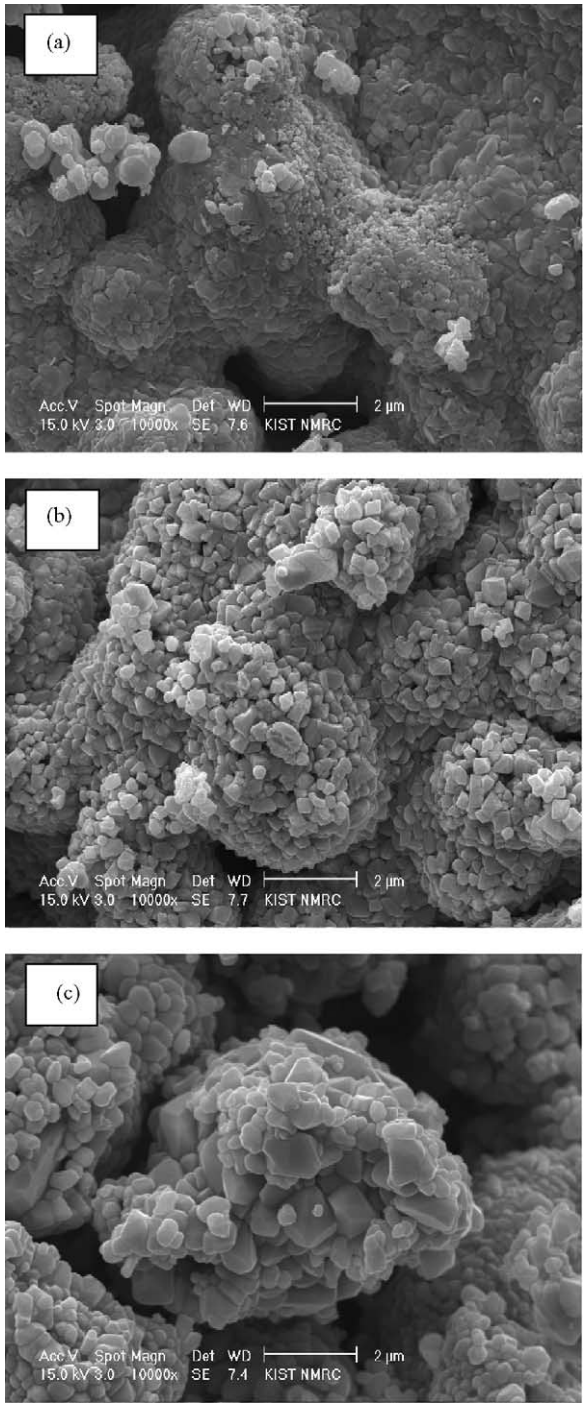

Fig. 9. SEM images of NiO and NiO–CoO electrodes after dissolution experiment in molten $Li_{0.62}K_{0.38}$ carbonate eutectics at 650 °C in 0.33% O_2–0.67% CO_2 atmosphere; NiO (a), 6 wt.% Co/NiO–CoO (b), 12 wt.% Co/NiO–CoO (c).

but no peaks for the hexagonal phases, such as $LiCoO_2$ and $Li(Co, Ni)O_2$ were observed [35].

The cubic lattice constants of the electrodes were obtained from the XRD analysis and they were plotted with Co contents in Fig. 11. The cubic lattice constants of the Li–Ni–Co–O compounds were smaller than that of Ni–Co–O

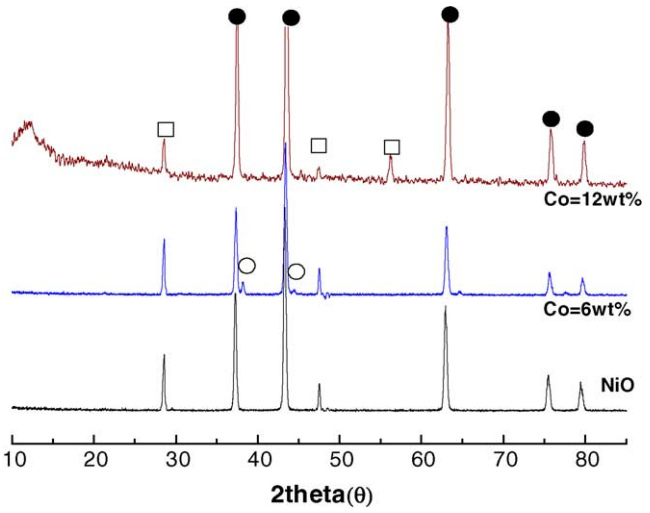

Fig. 10. XRD profiles of NiO and NiO–CoO electrodes after dissolution experiment; (Co, Ni)O (○), Li(Co, Ni)O(●), Si (□).

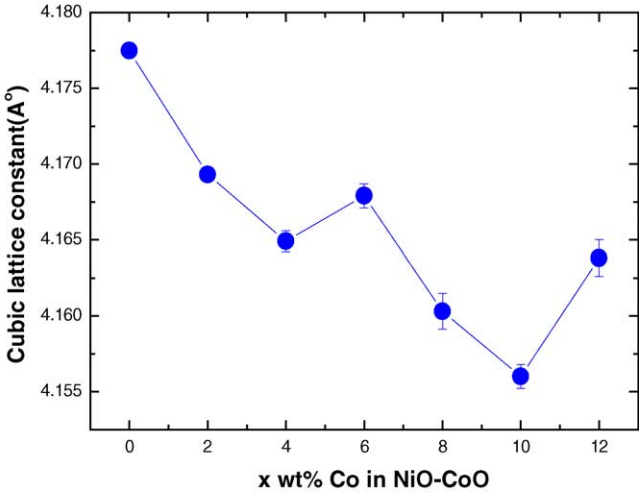

Fig. 11. Variation of cubic lattice constant with coated Co content.

compounds. According to the experimental results of Sato et al. [36] the lithiation of NiO and CoO caused the change in the lattice constants. They have reported that the cubic lattice constants of Li–Ni–O and Li–Co–O compounds decreased with increase in Li contents. Thus, the reduction in the cubic lattice constants of the NiO–CoO cathodes after the present dissolution experiment could be considered as the effect of incorporation of Li.

The cubic lattice constants shown in Fig. 11 decreased with increase of Co content in the Li–Ni–Co–O compounds after the dissolution experiment. Considering the lattice constants of the NiO–CoO electrodes before the dissolution experiment increased with the Co contents, the cubic lattice constants of Li–Ni–Co–O compounds were shrunk much more in the samples with higher Co contents. Li^+ ion, having a similar size to Ni^{2+}, incorporated into cubic phase NiO by filling the cation vacancy [37,38], and the vacancy concentration could be increased by the formation of NiO–CoO solid solution due to the valence difference between Ni^{2+} and Co^{3+} (in general, Co has 3+ valence in the present condition). Consequently, the high vacancy concentration of cations in NiO–CoO solid solution with high Co content caused the incorporation of Li in large amounts and thus, the cubic lattice constant of the Li–Ni–Co–O compound with high Co content was reduced.

In Fig. 12, the NiO solubility and the amount of lithium incorporated in the Li–Ni–Co–O compounds were plotted with Co contents. The amount of Li incorporated in the NiO–CoO solid solution was analyzed by AAS. As shown in the figure, the Ni solubility decreased with increase of Li contents in Li–Ni–Co–O compounds. The decrease of

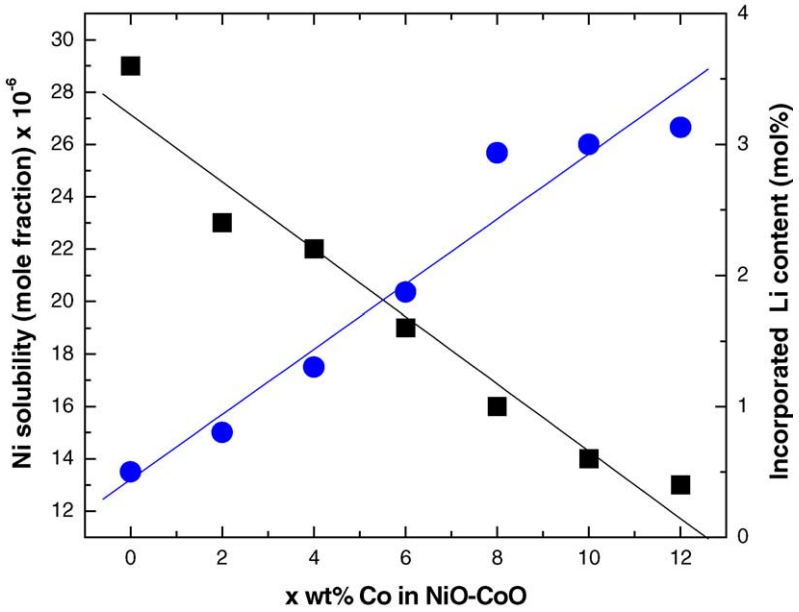

Fig. 12. Relationship between NiO solubility and amount of Li incorporated as a function of Co content in NiO–CoO electrodes.

Ni solubility by incorporation of Li has already reported in the literature [14], and the same trend was observed at the NiO–CoO system in the present study. The detailed mechanism of the decrease in Ni solubility by incorporation of Li is not clear yet. However, it might be possible that Li incorporation reduced the Gibbs free energy of NiO–CoO and thus, enhanced the stability of NiO–CoO. In general, the formation of the series solid solution with appropriate foreign atom content reduces the molar Gibbs free energy [39]. Consequently, it could be concluded that the formation of NiO–CoO solid solution promoted the incorporation of Li and thus, decreased the Ni solubility in the molten $(Li_{0.62}K_{0.38})_2CO_3$ eutectics.

4. Conclusion

The effect of Co on the suppression of NiO dissolution was investigated in molten $(Li_{0.62}K_{0.38})_2CO_3$ eutectics under standard cathode gas condition at 650 °C. The NiO–CoO electrode for MCFC was prepared by plating Co on the surface of a porous Ni electrode using a galvanostatic pulse plating technique followed by oxidation. In the Co plating process, the surface morphology of plated Co-layer depended on the pH value of the bath solution and homogenous Co distribution along the depth direction was observed for the sample prepared in the bath solution with a low pH value.

The results of the dissolution experiment showed that the NiO–CoO electrodes dramatically decreased the Ni solubility in the molten carbonate salt compared to the pure NiO electrode under the same conditions and within the same time. As P_{CO_2} increased, the Ni solubility of the NiO–CoO electrodes increased, but their sensitivity P_{CO_2} was smaller than the pure NiO cathode. However, the variation of P_{O_2} did not affect the Ni solubility. Similar to NiO and NiO–CoO, the Co solubility increased with P_{CO_2}. Consequently, the Ni and Co dissolution of the NiO–CoO electrodes followed the acidic dissolution mechanism.

The post analysis showed that the amount of Li incorporated into the NiO–CoO electrode increased with Co content. Also, the Ni solubility of NiO–CoO electrode decreased with increase of the amount of Li incorporated. Therefore, it was clear that the Ni solubility of NiO–CoO was closely related to the amount of Li incorporated and that the incorporation of Li could be promoted by the formation of a solid solution of NiO–CoO.

References

[1] M.L. Orfield, D.A. Shores, J. Electrochem. Soc. 136 (1989) 2862.
[2] N. Mortohira, T. Sensou, K. Yamauchi, K. Ogawa, X. Liu, N. Kamiya, K. Ota, J. Mol. Liq. 83 (1999) 95.
[3] S. Mitsushima, K. Matsuzawa, N. Kamiya, K. Ota, Electrochim. Acta 47 (2002) 3823.
[4] T. Fukui, S. Ohara, H. Okawa, T. Hotta, M. Naito, J. Power Sources 86 (2000) 340.
[5] T. Fukui, T. Hotta, H. Okawa, S. Ohara, M. Naito, K. Nogi, Electrochemistry 69 (2001) 335.
[6] T. Fukui, H. Okawa, T. Hotta, M. Naito, T. Yokoyama, J. Am. Ceram. Soc. 84 (2001) 233.
[7] P. Ganesan, H. Colon, B. Haran, R. White, B.N. Popov, J. Power Sources 111 (2002) 109.
[8] M. Yoshikawa, Y. Mugikura, T. Watanabe, T. Nishimura, T. Yagi, Y. Fujita, Electrochemistry 70 (2002) 183.
[9] B. Fang, H. Chen, J. Electroanal. Chem. 501 (2001) 128.
[10] B. Fang, C. Zhou, X. Liu, S. Duan, J. App. Electrochem. 31 (2001) 201.
[11] J. Soler, T. Gonzalez, M.J. Esudero, T. Rodrigo, L. Daza, J. Power Sources 106 (2003) 189.
[12] L. Daza, C.M. Rangel, J. Baranda, M.T. Casais, M.J. Martinez, J.A. Alonso, J. Power Sources 86 (2000) 329.
[13] L. Giorgi, M. Carewska, E. Simonetti, S. Scaccia, F. Croce, A. Pozio, Molten Salt Forum 1–2 (1993–1994) 285.
[14] M.J. Escudero, X.R. Novoa, T. Rodrigo, L. Daza, J. Power Sources 106 (2002) 196.
[15] P. Ganesan, H. Colon, B. Haran, B.N. Popov, J. Power Sources 115 (2003) 12.
[16] I. Bloom, M.T. lanagan, M. Krumpelt, J.L. Smith, J. Electrochem. Soc. 146 (1999) 1336.
[17] K. Takizawa, A. Hagiwara, Electrochemistry 69 (2001) 692.
[18] A. Lundblad, S. Schwartz, B. Bergman, J. Power Sources 90 (2000) 224.
[19] S. Freni, F. Barone, M. Puglisi, Int. J. Energy Res. 22 (1998) 17.
[20] A. Wijayasinghe, B. Bergman, C. Lagergren, J. Electrochem. Soc. 150 (2003) A558.
[21] J. Han, S.-G. Kim, S.P. Yoon, S.W. Nam, T.-H. Lim, I.-H. Oh, S.-A. Hong, H.C. Lim, J. Power Sources 106 (2002) 153.
[22] S.-G. Kim, S.P. Yoon, J. Han, S.W. Nam, T.-H. Lim, S.-A. Hong, H.C. Lim, J. Power Sources 112 (2002) 109.
[23] S.T. Kuk, Y.S. Song, K. Kim, J. Power Sources 83 (1999) 50.
[24] A. Durairajan, H.C.-M.B. Haran, R. White, B. Popov, J. Power Sources 104 (2002) 157.
[25] J.C. Puppe, N. Ibl, J. App. Electrochem. 10 (1980) 775.
[26] I. Uchida, T. Nishina, Y. Mugikura, K. Itaya, J. Electroanal. Chem. 206 (1986) 229.
[27] S. Scaccia, Talanta 49 (1999) 467.
[28] A. Bai, C.-C. Hu, Electrochim. Acta 47 (2002) 3447.
[29] E. Barrera, M.P. Pardave, N. Batina, I. Gonzalez, J. Electrochem. Soc. 147 (2000) 1787.
[30] JCPDF 47-1049.
[31] JCPDF 78-0431.
[32] K. Ota, S. Mitsushima, S. Kato, S. Asano, H. Yoshitake, N. Kamiya, J. Electrochem. Soc.
[33] C.-G. Lee, K. Yamada, T. Nishina, I. Uchida, J. Power Sources 62 (1996) 145.
[34] K. Yamada, I. Uchida, J. Electroanal. Chem. 385 (1995) 57.
[35] K. Takizawa, A. Hagiwara, J. Electrochem. Soc. 148 (2001) A1304.
[36] W.D. Kingery, H.K. Bowen, D.R. Uhlmann, Introduction to Ceramics, second ed., John Wiley & Sons, 1975, Chapter 6.
[37] T. Sato, J. Mater. Sci. Lett. 5 (1986) 552.
[38] M.S. Yazici, J.R. Selman, Solid State Ionics 124 (1999) 149.
[39] D. R. Gaskel, Introduction to the Thermodynamics of Materials, Chapter 9.